

# BOUNDARY-LAYER TURBULENCE ON A THERMALLY DISINTEGRATING SURFACE

Yu. A. Gostintsev, V. M. Zaitsev,  
and P. F. Pokhil

UDC 532.517.4:66.092.9

We describe the experimental investigation of transition from laminar to turbulent flow in the boundary layer on a thermally disintegrating surface.

The experiments involved determination of the linear rate of gasification for models of polymethyl methacrylate or epoxy resin (ED6 + 10% polyethylenepolyamine) in a high-temperature chemically neutral flow of products of combustion (average molecular weight for the gas, approximately 30,  $T^0 \approx 1200^\circ\text{K}$ , dynamic viscosity  $\mu = 5 \cdot 10^{-4}$  poise). Using microthermocouples, in a number of the experiments we measured the temperature profiles in the boundary layer over a disintegrating surface. The tungsten-rhenium thermocouples were  $30 \mu\text{m}$  in size. The models were formed of short cylindrical tubes 40 mm in length, with channel diameters of 15 mm and 10 mm.

Since the test models are considerably shorter than the thermal and hydrodynamic flow-stabilization segments in the tube, we can assume that the increase in the boundary layer along the channel wall in these tests proceeds as on a flat ablating plate, while the variation in the temperature and velocity of the main gas flow is insignificant over the length of the specimen because of the transfer of heat and mass between the flow and the walls. A laminar boundary flow is formed near the tube inlet; the flow in this layer loses stability at some point downstream and becomes turbulent.

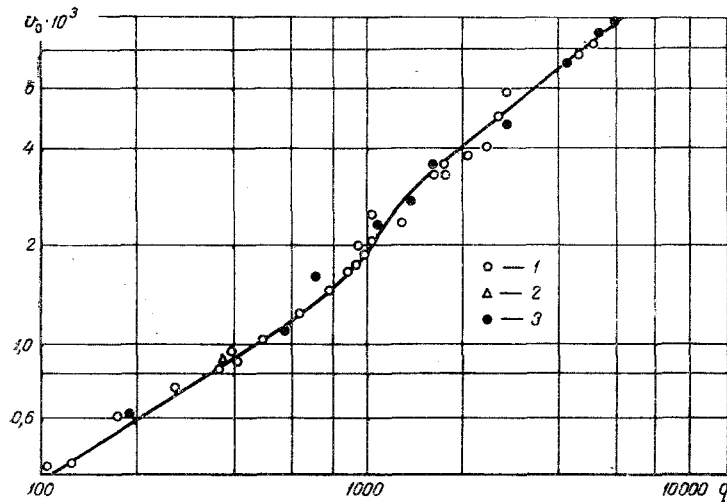


Fig. 1. Linear gasification rate  $v_0$  (m/sec) for the models as a function of the density ( $\text{kg/m}^2 \cdot \text{sec}$ ) for the mass flow in the channel: 1) polymethyl methacrylate,  $d_0 = 15$  mm; 2) polymethyl methacrylate,  $d_0 = 10$  mm; 3) epoxy resin,  $d_0 = 15$  mm.

Institute of Chemical Physics, Academy of Sciences of the USSR, Moscow. Translated from *Inzhenerno-Fizicheskii Zhurnal*, Vol. 16, No. 5, pp. 773-779, May, 1969. Original article submitted July 10, 1968.

© 1972 Consultants Bureau, a division of Plenum Publishing Corporation, 227 West 17th Street, New York, N. Y. 10011. All rights reserved. This article cannot be reproduced for any purpose whatsoever without permission of the publisher. A copy of this article is available from the publisher for \$15.00.

In these experiments we were able to determine the appearance of turbulence in the boundary layer both from the change in the relationship between the ablation rate (i.e., in the intensity of heat transfer) and the density of the gas flow in the channel (see Fig. 1, where the measurement was carried out at the tube outlet), and from the appearance of turbulent fluctuations in temperature in the boundary layer.

We see from Fig. 1 that at low flow densities or, what is the same, for low Reynolds numbers, the boundary layer on the disintegrating surface remains laminar, and the law governing the transfer of heat between the gas and the wall is subject to the function  $Nu \sim Re^{0.60}$ . For large Reynolds numbers the boundary layer is turbulent and the heat-transfer function is of the form  $Nu \sim Re^m$ , where  $m$  is a parameter varying from 0.8 to 1.0 with an increase in  $Re$  [1]. In the intervening region of  $Re$  values the flow in the boundary layer changes from laminar to turbulent.

The steady flow of a viscous heat-conducting gas in a laminar boundary layer is described by the equations

$$\frac{\partial}{\partial x}(\rho u) + \frac{\partial}{\partial y}(\rho v) = 0, \quad (1)$$

$$\rho u \frac{\partial u}{\partial x} + \rho v \frac{\partial u}{\partial y} = \frac{\partial}{\partial y} \left( \mu \frac{\partial u}{\partial y} \right) - \frac{\partial p}{\partial x}, \quad (2)$$

$$c_p \left( \rho u \frac{\partial T}{\partial x} + \rho v \frac{\partial T}{\partial y} \right) = \frac{\partial}{\partial y} \left( \lambda \frac{\partial T}{\partial y} \right) + \mu \left( \frac{\partial u}{\partial y} \right)^2 + u \frac{\partial p}{\partial x}. \quad (3)$$

Having introduced the thicknesses of the hydrodynamic ( $\delta$ ) and thermal ( $\Delta$ ) layers, and having integrated (2) and (3) over the transverse coordinate  $y$ , we obtain the equations of momentum and energy for the laminar boundary layer on a disintegrating plate [2]:

$$\frac{d}{dx} \int_0^{\delta} \rho u (u_1 - u) dy + \frac{du_1}{dx} \int_0^{\delta} (\rho_1 u_1 - \rho u) dy = \rho_0 v_0 u_1 + \left( \mu \frac{\partial u}{\partial y} \right)_0, \quad (4)$$

$$\frac{d}{dx} \int_0^{\Delta} \rho u c_p (T_1 - T) dy + \frac{d(c_p T_1)}{dx} \int_0^{\Delta} u (\rho_1 - \rho) dy + \int_0^{\Delta} \mu \left( \frac{\partial u}{\partial y} \right)^2 dy = \rho_0 v_0 c_p (T_1 - T_0) + \left( \lambda \frac{\partial T}{\partial y} \right)_0. \quad (5)$$

Since we can assume in these experiments that  $dT_1/dx = du_1/dx = 0$  because of the limited length of the model and the low velocities of product motion, and since we can neglect the compressibility of the gas and the heat release resulting from viscous dissipation, from (4) and (5) we easily obtain

$$\frac{d}{dx} \int_0^{\delta} \rho u (u_1 - u) dy = \rho_0 v_0 u_1 + \left( \mu \frac{\partial u}{\partial y} \right)_0, \quad (6)$$

$$\frac{d}{dx} \int_0^{\Delta} \rho u c_p (T_1 - T) dy = \rho_0 v_0 c_p (T_1 - T_0) + \left( \lambda \frac{\partial T}{\partial y} \right)_0. \quad (7)$$

The boundary conditions of the problem have the form

$$\begin{aligned} u &= u_1, \quad \frac{\partial u}{\partial y} = \frac{\partial^2 u}{\partial y^2} = 0 \text{ when } y = \delta, \\ T &= T_1, \quad \frac{\partial T}{\partial y} = \frac{\partial^2 T}{\partial y^2} = 0 \text{ when } y = \Delta, \\ u &= 0, \quad T = T_0, \quad \frac{\partial}{\partial y} \left( \lambda \frac{\partial T}{\partial y} \right)_0 = c_p \rho_0 v_0 \left( \frac{\partial T}{\partial y} \right)_0, \\ &\frac{\partial}{\partial y} \left( \mu \frac{\partial u}{\partial y} \right)_0 = \rho_0 v_0 \left( \frac{\partial u}{\partial y} \right)_0 \text{ when } y = 0 \end{aligned}$$

(the two last conditions have been derived from (2) and (3) for the case of flow without a gradient). For the approximate solution of the original system of equations (6) and (7) we will employ the Pohlhausen method.

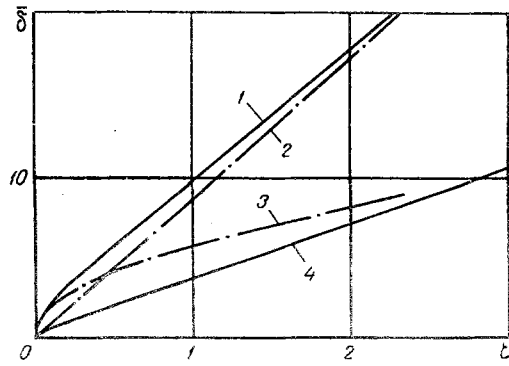


Fig. 2

Fig. 2. 1) Solution for Eq. (10); 2) asymptote for  $\bar{\delta}$  (for  $\zeta \gg 1$ ); 3) solution for (10) in the absence of injection; 4) displacement thickness.

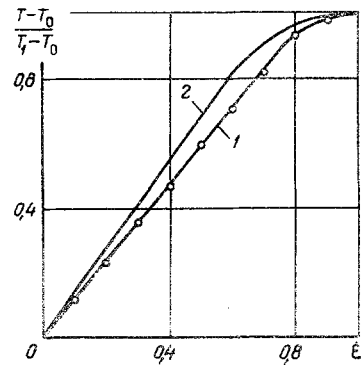


Fig. 3

Fig. 3. Temperature profiles – theoretical (2) and experimental (1) – for  $\zeta = 2.4$ .

We will specify the velocity and temperature profiles in the form of a polynomial of fourth degree, satisfying the boundary conditions

$$\frac{u}{u_1} = \frac{6}{6+\delta} (2\eta + \eta^4 - 2\eta^3) + \frac{\bar{\delta}}{6+\delta} (6\eta^2 - 8\eta^3 + 3\eta^4), \quad (8)$$

$$\frac{T-T_0}{T_1-T_0} = \frac{6}{6+\Delta} (2\xi - 2\xi^3 + \xi^4) + \frac{\bar{\Delta}}{6+\Delta} (6\xi^2 - 8\xi^3 + 3\xi^4). \quad (9)$$

Then, after substitution of (8) into (6), for the dimensionless thickness of the hydrodynamic boundary layer we will have

$$\frac{d\bar{\delta}}{d\zeta} \frac{888\bar{\delta} + 476\bar{\delta}^2 + 72\bar{\delta}^3 + 4\bar{\delta}^4}{432 + 360\bar{\delta} + 120\bar{\delta}^2 + 18\bar{\delta}^3 + \bar{\delta}^4} = 35, \quad (10)$$

where

$$\bar{\delta} = \delta \frac{\rho_0 v_0}{\mu}, \quad \eta = \frac{y}{\delta}, \quad \xi = \frac{y}{\Delta}, \quad \zeta = x \frac{(\rho_0 v_0)^2}{\mu \rho_1 u_1}.$$

Figure 2 shows the solution for (10) in the form of  $\bar{\delta}$  as a function of  $\zeta$ . We see that for small  $\zeta$  the boundary layer increases exactly as on a solid surface (curve 3), while for  $\zeta \gg 1.0$  the law governing its increase becomes linear (curve 2). Introducing the boundary-layer displacement thickness into our consideration, i.e.,

$$\frac{\bar{\delta}_*}{\bar{\delta}} = \int_0^1 (1 - u/u_1) d\eta = \frac{9 + 2\bar{\delta}}{5(6 + 2\bar{\delta})},$$

we find that near the leading edge of the plate  $\delta_* = 1.75 (x\mu/\rho_1 u_1)^{1/2}$ , while at a distance from that edge, where the effect of viscosity becomes small and the formation of the boundary layer is governed primarily by the additional influx of mass from the wall, we have  $\delta_* = 3.5 \rho_0 v_0 x / (\rho_1 u_1)$ . The general function  $\bar{\delta}_*(\zeta)$  is shown in Fig 2 (curve 4). Bearing in mind that the mass rate  $\rho_0 v_0$  for the gasification of a thermally disintegrating body is determined by the magnitudes of the heat flow to the wall and the total heat of phase conversion  $H$ , it is not difficult to find that near the edge

$$\rho_0 v_0 = \text{const} \frac{\lambda(T_1 - T_0)}{H} \sqrt{\frac{\rho_1 u_1}{x\mu}}, \quad (11)$$

and at a distance from the edge,

$$\rho_0 v_0 = \text{const} \sqrt{\frac{\lambda(T_1 - T_0)}{H}} \sqrt{\frac{\rho_1 u_1}{x}}. \quad (12)$$

We see that in the laminar flow regime in the boundary layer the mass flow rate for ablation is proportional to the square root of the ratio of the density ( $\rho_1 u_1$ ) of the main flow to the distance ( $x$ ) from the inlet. The data in Fig. 1 confirm this conclusion, although experimentally we find a somewhat stronger relationship between  $\rho_0 v_0$  and  $\rho_1 u_1$ . Measurement of temperature in the boundary layer also confirms the possibility of using the above calculation to derive qualitative relationships. Thus, Fig. 3 (for purposes of comparison) shows the dimensionless temperature profiles in the boundary layer over a disintegrating surface for  $\zeta = 2.40$ : calculated from (7) and (9) for a Prandtl number  $Pr = 1$  (curve 2) and measured experimentally (curve 1).

Generalization of the data for the temperature measurements and the measured ablation-rate functions enables us to determine the critical value of the Reynolds number. It developed that transition to turbulent flow in the boundary layer on an ablating surface begins with the Reynolds number for the local displacement thickness  $\delta_*$ , i.e.,

$$Re_* = \frac{\rho_1 u_1 \delta_*}{\mu} = 1300 - 1500.$$

The resulting value of the critical Reynolds number is somewhat greater than the value of  $Re_*$  for the isothermal streamlining of a flat impermeable plate [3]. This circumstance can probably be explained by the fact that the destabilization of the boundary layer – because of the influx of additional mass from the ablating walls – is weaker than the stabilizing effect of gas cooling within the layer.

Indeed, for the gradient-free flow of a hot gas over a thermally disintegrating surface, from the equation of motion, at the wall we find

$$\rho_0 v_0 \left( \frac{\partial u}{\partial y} \right)_0 = \frac{\partial}{\partial y} \left( \mu \frac{\partial u}{\partial y} \right)_0. \quad (13)$$

Hence, assuming the function  $\mu/\mu_0 = T/T_0$  for the viscosity of the gas and taking  $Pr = 1$ , it is easy to find the expression for the slope of the velocity profile, whose sign determines the stability of the flow in the boundary layer:

$$\left( \frac{\partial^2 u}{\partial y^2} \right)_0 = - \left( \frac{\partial u}{\partial y} \right)_0 \left( \frac{\partial T}{\partial y} \right)_0 \frac{1}{T_0} \left( 1 - \frac{cT_0}{H} \right). \quad (14)$$

Since  $cT_0/H < 1$ , it follows from (14) that the stabilizing effect of the transfer of heat between the gas and the wall in the case of a thermally disintegrating surface is stronger than the destabilizing effect of the additional influx of mass from the walls.

In this connection, experimentally we observed a slight constriction of the transition to turbulence in the boundary layer on the ablating plate, as compared with the streamlining of a nondisintegrating surface. An analogous effect was observed in flight tests of disintegrating cones [4].

With a change in the nature of the flow in the boundary layer there is a pronounced change in the form of the wall being swept. In the region of Reynolds numbers in which the boundary layer remains laminar, the surface of the model after the test is smooth, with no apparent irregularities. After complete turbulization of the boundary layer, virtually the entire surface of the channel becomes irregular, cellular, and pitted [1]. A motion-picture film of the process involved in the appearance and development of the perturbations in the boundary layer on the ablating surface makes possible a detailed comparison of the patterns of transition on solid and disintegrating surfaces. Such a motion-picture filming operation proved to be possible because the entire structure of the flow in the boundary layer is reflected at the surface when a thermally disintegrating material is streamlined by a hot gas (regardless of the particular physical process that is involved, i.e., ablation, sublimation, or combustion). For this we need only make certain that the exposure for the entire vortex system in the layer (the intermittance time  $\tau_0$ ) is sufficient to produce a thermal impression. We know that the characteristic relaxation time for the heated layer of a body is given by  $\tau_1 \sim \kappa/u_0^2$  and in the transition region, in the streamlining of polymethyl methacrylate, it is  $\tau_1 \sim 10^{-1}$  sec, i.e., it is of the same order of magnitude as the intermittance time  $\tau_0$ . (According to the measurements in [5], at flow velocities of 10–25 m/sec the frequency of flow intermittance in the boundary layer is 10–20 Hz.) This makes clear the possibility of studying the transition from the roughness pattern on the surface of a disintegrating body.

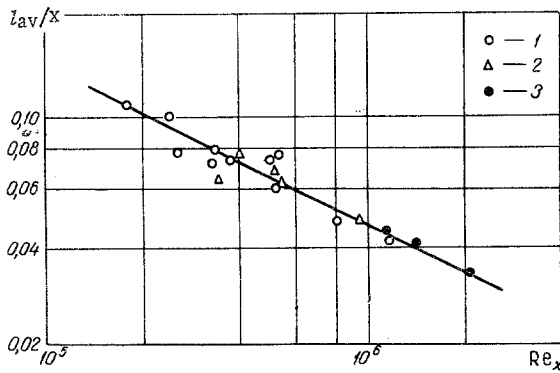


Fig. 4. Relative average roughness dimension on a streamlined surface as a function of the Reynolds flow number: 1) polymethyl methacrylate; 2) epoxy resin; 3) polymethyl methacrylate in swirled flow.

depressions function in the same manner as rough spots in the streamlining of a solid plate and promote the generation of local turbulent pulsations in the boundary layer. However, such roughness on a disintegrating surface, unlike the case with a solid wall, interacting with the microvortices in the boundary layer, itself undergoes change, i.e., the cells increase in size to a certain point, forming a chain of irregularities, which are oriented in the direction of the flow. Regardless of which of the described mechanisms leads to the transition from the laminar to turbulent flow in the boundary layer (usually both of the mechanisms act simultaneously), the linear dimension  $l$  of the cells completely developed on the specimen is determined by the dimensions of the microvortices and is proportional to the thickness of the boundary layer, i.e.,

$$\frac{l}{x} \sim \frac{\rho_0 u_0}{\rho_1 u_1} \sim \sqrt{\frac{\mu c(T_1 - T_0)}{\rho_1 u_1 x H}} = Re_x^{-1/2} \sqrt{\frac{c(T_1 - T_0)}{H}}$$

Figure 4 shows the experimental relationship between the average relative cell dimension  $l/x$  and the  $Re_x$  number, found for the ablation of specimens made of polymethyl methacrylate and epoxy resin.

It is interesting that in studying the decomposition of the channel walls of a cylinder in a highly swirled flow [1] it is not axisymmetric perturbations that arise initially in the transition region, but rather perturbations of the Taylor–Goertler wave type, oriented along the streamlines. However, the structure of the cells and their dimensions, as before, are determined by the state of the boundary layer (see Fig. 4).

Preliminary investigation of transition to turbulent flow at the surfaces of sublimating materials without a melt film (for example,  $NH_4ClO_4$ ) demonstrated that the characteristic dimensions for the cells formed at the wall are determined by an analogous dependence on the  $Re$  number, and the mechanism for the appearance of turbulent pulsations in the boundary layer is similar to the one in the streamlining of a smooth surface, if the initial particle dimensions for the compressed material are small, and it is similar to the mechanism for transition on a rough plate, if the particle dimensions are sufficiently large.

#### NOTATION

$c$	is the heat capacity of the disintegrating body;
$\mu$	is the dynamic viscosity of the gas;
$\rho$	is the density;
$u$	is the axial flow velocity of the gas;
$v_0$	is the linear gasification rate;
$q = \rho_1 u_1$	is the mass density of the flow;
$T$	is the temperature;
$\delta, \Delta$	are, respectively, the thicknesses of the hydrodynamic and thermal boundary layers;
$\lambda$	is the thermal conductivity of the gas;
$H$	is the total heat of phase conversion;
$l$	is the linear roughness dimension at the streamlined surface;

It developed, as in the streamlining of a rigid surface [5], that the initial indicators of the instability of the laminar boundary layer are found in the form of a series of two-dimensional axisymmetric perturbations such as Tollmien–Schlichting waves. With the passage of time, these waves are intensified, they become three-dimensional and unstable, and as a consequence a more or less ordered structure is formed from the vortex cells, reminiscent in shape to the horseshoe vortices of Theodorsen. These vortices subsequently disintegrate, generating irregular turbulent pulsations.

The motion-picture films of the process revealed yet another possible mechanism for the appearance of turbulence in the boundary layer. With the existence of inhomogeneities in the material of the model (for example, gas bubbles) at the beginning of the test, prior to the formation of a viscous melt film at the surface of the specimen, small hemispherical pits appear. These de-

Nu is the Nusselt number;  
Re is the Reynolds number;  
Subscript 0 gives the values of the parameters at the wall;  
Subscript 1 identifies the parameters in the flow, outside the boundary layer.

#### LITERATURE CITED

1. Yu. A. Gostintsev et al., *Izv. Akad. Nauk SSSR, Mekhanika Zhidkosti i Gaza*, No. 5 (1967).
2. *Turbulent Flows and Heat Transfer* [Russian translation], IL (1963).
3. H. Schlichting, *The Appearance of Turbulence* [Russian translation], IL (1962).
4. M. Wilkins and M. Tauber, *Raketnaya Tekhnika i Kosmonavtika*, No. 8 (1966).
5. C. F. Knapp and P. Roache, *AIAA Journ.*, 6, No. 1 (1968).